보건학석사 학위논문

Antimicrobial Properties of Novel Magnetic -Silica-Silver Nanoparticle Composites

새로운 Magnetic-Silica 은나노 복합체의 미생물 저감 효과

2012년 08월

서울대학교 보건대학원

환경보건학과 환경보건학 전공

박 성 준

Antimicrobial Properties of Novel Magnetic -Silica-Silver Nanoparticle Composites

새로운 Magnetic-Silica 은나노 복합체의 미생물 저감 효과

지도교수 고 광 표

이 논문을 보건학 석사학위 논문으로 제출함

2012년 8월

서울대학교 보건대학원

환경보건학과 환경보건학 전공

박 성 준

박성준의 석사학위논문을 인준함

2012년 8월

위 원 장 최 경 호 (인)

부위원장 조 경 덕 (인)

위 원 고 광 표 (인)

Abstract

Antimicrobial Properties of Novel Magnetic -Silica-Silver Nanoparticle Composites

SungJun Park

Dept. of Environmental Health

The Graduate School of Public Health

Seoul National University

Silver nanoparticles (AgNPs) have been long considered as a useful tool for controlling various pathogens. However, the large surface-area-to-volume ratio and the cytotoxicity of AgNPs are associated with several adverse health effects and ecological hazards. In this study, we tested novel AgNP composites containing a magnetic core and a silica layer (Ag@MSCs). These composites are more effective in inactivating various microorganisms and possibly recovered. First, we evaluated the antimicrobial capabilities of the Ag@MSCs against both bacteria (*E. coli* CN13 and *B. Subtilis*) and bacteriophages (MS2 and ΦX174). Moreover, the Ag@MSCs were exposed to a wide range of pH levels, tap water, and surface water to assess the antimicrobial effects under different environmental conditions. Among the different types of Ag@MSCs, 30Ag@MSC, which contained 30nm monodispersed AgNPs on the outer surface of the silica

layer, showed the strongest effect. The highest concentration of 30Ag@MSCs, approximately 7.13×10^9 particles/ml, exhibited more than 5-log reduction of bacteria and 2-log reduction of phages within 1 hour. Also, regardless of the condition, the 30Ag@MSCs maintained their strong efficacy. These results suggest that the proposed Ag composites can be used in various environmental settings and recovered within a few minutes using a strong magnet to reduce the potential harmful effects on human health and the environment.

Key words: Silver, Nanoparticle, Composite, Microorganism, Antimicrobial agents

Student No. 2010-23783

Contents

List of Tables

List of Figures

I. Introduction

Nano-sized materials have unique physiochemical properties compared to larger materials due to their high surface-to-volume-ratio (18). With recent advances in nanotechnology, nanomaterials are receiving attention worldwide due to their various practical uses in medicine, biotechnology, and controlling pathogens (18, 25). Currently, it is possible to control the shape and size of nanomaterials and to conjugate specific functional groups on the surface of a nanomaterial for interactions with certain proteins and for intracellular uptake depending on the purpose (5, 26, 33). Normally, the field of biotechnology uses nanoparticles ranging from 10 to 500nm in size (18).

Among these, silver nanoparticles (AgNPs) have been studied actively as an antimicrobial agent (23). Historically, silver has been used in the creation of fine cutlery, for ornamentation, and in therapeutic agents. Silver compounds such as silver sulfadiazine and certain salts have been used as wound care products and as treatments for infectious diseases due to their microbicidal effect (12, 23). Furthermore, recent studies have revealed that AgNPs are very effective for inactivating various types of bacteria and viruses (9, 10, 11, 14, 28). AgNPs are known to interact directly with thiol or phosphate groups of biomolecules, including proteins and nucleic acids. They have also been shown to generate reactive oxygen species (ROS), causing microbial membrane and DNA damage. The size, shape and concentration of AgNPs are also important factors which affect their antimicrobial capabilities (9, 11, 19, 21, 27, 32).

However, there are several problems when using AgNPs to control pathogens. First, the use of common monodispersed AgNPs can lead to particle-particle aggregation due to their small size

and large surface area, which reduces their effectiveness (12). Also, a high concentration of AgNPs shows various cytotoxic effects. Moreover, it is impossible to recover monodispersed AgNPs after their use in the environment (7, 20, 22, 32). Therefore, the misuse or overuse of AgNPs can cause serious adverse health effects while also representing on ecological hazard.

In this study, we designed novel AgNP composite with a magnetic core and a silica layer. Different sizes of AgNPs were tightly fixed in a silica layer to prevent particle-particle aggregation. The magnetic core of the composites enabled us to recover the composites within a few minutes using a strong magnet. Then, we evaluated the antimicrobial activity of the composites against both bacteria *(E. coli* CN13 and *B. Subtilis*) and bacteriophages (MS2 and ΦX174) and assessed their antimicrobial effects after exposure to different environmental conditions, including a wide range of pH levels, tap water, and surface water. In addition, we determined the antimicrobial mechanisms of the AgNP composite through experiments to investigate the relationship between the generated ROS and the antimicrobial effect and to take TEM images of *E. coli* CN13 with composites in various time points.

II. Materials and Methods

1. Characterization of magnetic-silica-silver nanoparticle composites

All of the magnetic-silica-silver nanoparticle composites (Ag@MSCs) were provided by the Molecular Recognition Research Center of the Korea Institute of Science and Technology (KIST), Seoul, Korea. Briefly, Ag@MSC consisted of three parts (Figure 1). A magnetic core was placed at the center of each composite and coated in a silica layer. Then, 10, 20, and 30 nm monodispersed AgNPs or hydroxyl groups (-OH) as a control were tightly fixed to the outer surface of the silica layer shown by the Transmission electron microscopy (TEM) images (Figure 2). Triply-distilled water was used to make the Ag@MSC solution and the initial concentration of the Ag@MSC solution was approximately 7.13×10^9 particles/ml (Table 1). The completed Ag@MSC solution was stored at room temperature (25℃) in a dark place.

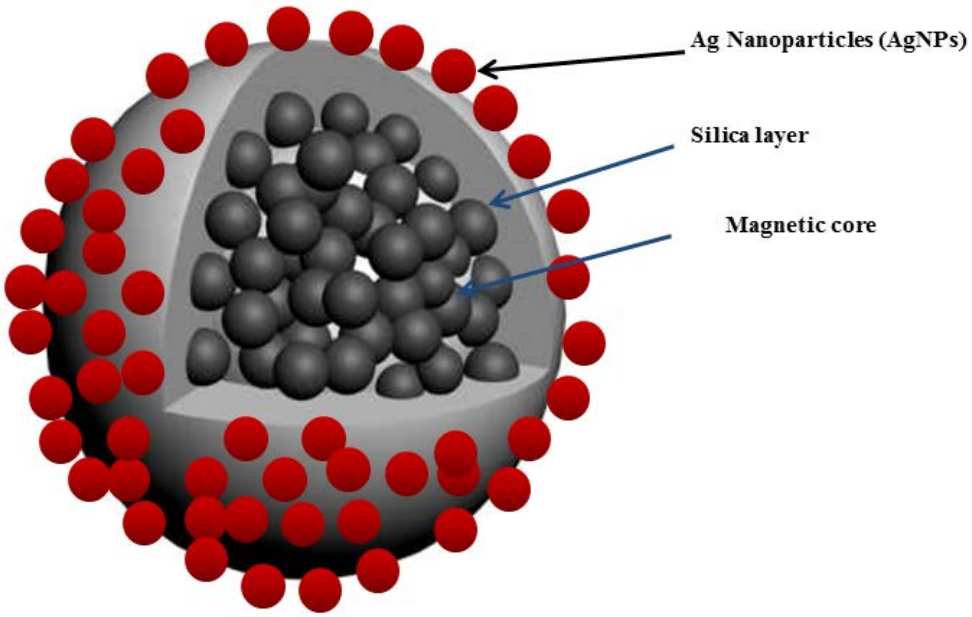

Figure 1.

The structure of Magnetic-Silica-AgNP composites (Ag@MSC).

Table 1. AgNp composite samples used in this study

Samples	**Number-concentration**[a]	**Silver concentration (ppm)**[c]	**Number of AgNPs/MSC**	**Surface area of one particle (nm^2)**[d]
10Ag@MSC[b]	7.13×10^9	28.75	1.74×10^3	3.07×10^5
20Ag@MSC	7.13×10^9	137.5	1.04×10^3	7.35×10^5
30Ag@MSC	7.13×10^9	200	1.89×10^2	5.34×10^5

[a] Number of particles per 1ml triply-distilled H_2O (6)

[b] MSC is the abbreviation of Magnetic-Silica-Composites and 10Ag@MSC, 20Ag@MSC, and 30Ag MSC contained 10nm, 20nm, and 30nm monodispersed AgNPs respectively.

[c] Ag concentration was obtained from Advanced Analysis Center of KIST using Atomic Absorption Spectrometer (AAS) and Inductively Coupled Plasma (ICP) analysis.

[d] Calculated by the following formula: Surface area of one AgNP ($4\pi r^2$) x Number of AgNPs/MSC

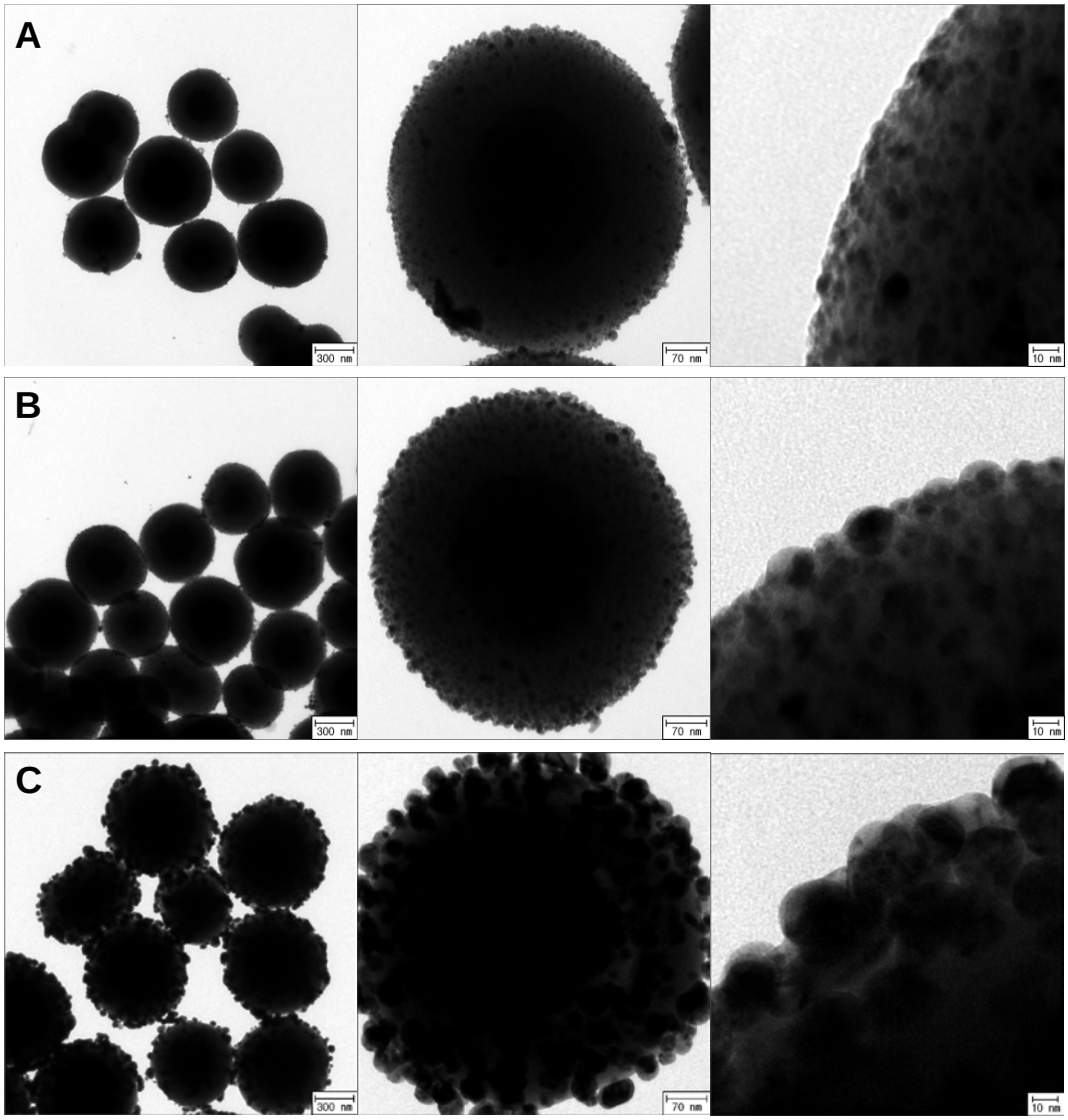

Figure 2.

TEM images of the Ag@MSC samples. A) 10Ag@MSC , B) 20Ag@MSC, and C)30Ag@MSC contained 10nm, 20nm, and 30nm monodispersed AgNPs respectively.

2. Preparation of target microorganisms

Two strains of *Escherichia coli* (*E. coli*), CN13 (ATCC No. 700609) and C3000 (ATCC No. 15597), were cultured in tryptic soy broth (TSB, BD Bacto™, USA) as previously described (4). After overnight culturing at 37℃, the concentration of the *E. coli* stocks was measured using serial dilution and the colony counting method. In addition, *Bacillus subtilis* (*B. subtilis*, ATCC No. 6633) was cultured in nutrient broth (NA, BD Dicfo™, USA) at 35℃ and the concentration was measured as mentioned above (24). All of the bacteria stocks were aliquoted and stored at 4℃.

Bacteriophage MS2 (ATCC No. 15597-B1) and ΦX174 (ATCC 13706-B1) were propagated using the single agar layer (SAL) method and *E. coli* C3000 as the host bacteria (2, 30). After overnight culturing at 37℃, the phages were purified from phosphate-buffered saline (PBS)-washed *E. coli* lysates (13). Briefly, an equal volume of chloroform was added to the lysates followed by centrifugation (30 min, 4℃, 4000 x g). Then, the supernatant, used as the phage stocks, was recovered and stored at -80℃.

3. Antimicrobial effects of Ag@MSCs

To assess the antimicrobial activity of Ag@MSCs depending on the concentrations used, approximately 1×10^6 colony forming unit (CFU)/ml of bacteria (*E. coli and B. subtilis*) or 1×10^6 plaque forming unit (PFU)/ml of phages (MS2 and ΦX174) were treated with three different concentrations of 10, 20 and 30Ag@MSCs (7.13×10^9 particles/ml, 7.13×10^8 particles/ml, and 7.13×10^7 particles/ml) in a shaking incubator (1 hr, 25℃, 150 rpm). 7.13×10^9 particles/ml of OH@MSCs were used as a control. Following the treatment, colony counting and SAL methods were used to measure surviving bacteria and phages, respectively. Three to 300 colonies or plaques were counted on the plates.

For measuring the interaction between antimicrobial effects and reaction times, approximately 1×10^6 CFU/ml or 1×10^6 PFU/ml of each microorganism were treated with 7.13×10^9 particles/ml of the composites in a shaking incubator (25℃, 150 rpm). After 1, 3, and 6 hr of incubation, the surviving microorganisms were measured by the colony counting and SAL methods.

4. Effect of exposure to various pH conditions towards Ag@MSCs

To understand the effect of pH exposure, 7.13×10^9 particles/ml of 30Ag@MSCs were exposed to acid (pH 2.0 and 5.0) or alkali (pH 9.0 and 12.0) conditions created by the addition of 0.1 N HCL or 0.1 N NaOH in a shaking incubator (10 min, 25℃, 150 rpm), as previously described with some modifications (31). pH values were measured using an Orion 3-Star Benchtop pH meter (Thermo Fisher Scientific, USA). After neutralization, 30Ag@MSCs were recovered from solution using a strong magnet and re-suspended in triply-distilled water at the same initial concentration. 1×10^6 CFU/ml of bacteria or 1×10^6 PFU/ml of phages were mixed with the exposed and unexposed (control, pH 7.6) 30Ag@MSCs in a shaking incubator (10 min, 25℃, 150 rpm) and measured by the colony counting and SAL methods.

Additionally, TEM images of the 30Ag@MSCs after exposure to pH 2.0, 7.0 and 12.0 were captured using a Libra® energy filtering transmission electron microscope (EFTEM, Carl Zeiss Co. Ltd, Korea) at the National Instrumentation Center for Environmental Management (NICEM), Seoul National University.

5. Antimicrobial activities of Ag@MSCs in tap and surface water

Surface water was sampled in July 2011 at the Hangang Park Yeouido Area, located at the Han River, Seoul, Korea. All water samples were collected in 1 L sterilized bottles and stored at 4℃ before being examined. Water analysis, according to Korean standards for drinking water quality, was carried out by Wendi-Bio Inc. (http://www.wendibio.com), who acquired the license for analyzing drinking water from the Ministry of Environment, Korea. Before treating the water with the microorganisms, 7.13×10^9 particles/ml of 30Ag@MSCs were added to the tap and surface water in a shaking incubator (10 min, 25℃). Two types of surface water, filtered with 0.22㎛ syringe filter (Millipore Millex®, USA) and non-filtered, were used and the background concentration of microorganisms was measured by the colony counting and SAL methods prior to the assay. Subsequently, 1×10^6 CFU/ml or 1×10^6 PFU/ml of microorganisms were added to the treated and untreated (control) 30Ag@MSCs in a shaking incubator (1 hr, 25℃, 150 rpm) and measured by the colony counting and SAL methods.

6. Antimicrobial Mechanisms of Ag@MSCs

A. The relationship between ROS generation and antimicrobial activity

To determine the effect of free radicals including ROS, approximately 1×10^6 CFU/ml of *E. coli* CN13 was treated with 7.13×10^9 particles/ml of 30Ag@MSCs and the antioxidant N-Acetyl-Cysteine (NAC, Sigma-Aldrich Korea) as previously described (9). Two concentrations of NAC, 1 mM and 0.1 mM) were selected, which did not affect the *E. coli* concentration. After shaking in the incubator (1hr, 25℃, 150 rpm), the concentration of the surviving bacteria was measured by colony counting. All experiments were performed in triplicate.

In addition, ROS generation within the cell, caused by the Ag@MSCs, was determined with 5-(and-6)-carboxy-2′,7′-dichlorodihydrofluorescein diacetate (carboxy-H2DCFDA, Invitrogen Molecular Probes™, USA) as previously described with minor modifications (8). After incubating for 30 min in PBS containing 10㎛ carboxy-H2DCFDA at 37℃, *E. coli* was washed and treated with 7.13×10^9 particles/ml of 10, 20, and 30 Ag@MSCs in a shaking incubator (30 min, 25℃, 150 rpm). The fluorescence of the samples was measured with an Infinite® 200 pro multimode reader (Tecan Trading AG, Switzerland) at 495nm excitation wavelength and 520nm emission wavelength, and the fluorescence intensity was described as the fold increase compared to the control (OH@MSC).

B. Interaction between microbial membrane and Ag@MSCs

To understand the interaction between the microbial membrane and Ag@MSCs, *E. coli* CN13 was treated with 30Ag@MSCs for 10 min, 1 hr, and 24 hr in a shaking incubator (25℃, 150 rpm).

Subsequently, a drop of sample containing *E. coli* and 30Ag@MSCs was deposited on a grid and was negative-stained with 2% (W/V) phosphotungstic acid (PTA) as previously described (16). The grid samples were analyzed with a Libra® EFTEM at the National Instrumentation Center for Environmental Management (NICEM), Seoul National University.

7. Statistical analysis

The data were expressed as the mean ± standard deviation(SD) for at least three independent experiments. Wherever appropriate, the data were analyzed with one-way analysis of variance (ANOVA) or Kruskal-Wallis one-way ANOVA followed by post hoc Dunnett's test for multiple comparisons. A P value less than <0.05 was considered statically significant. SPSS® statistics for windows ver. 19.0 (IBM®, USA) and Sigmaplot for windows ver. 12.0 (Systat software Inc, USA) were used for the statistical analysis.

III. Results

1. Antimicrobial effects of Ag@MSCs

The antimicrobial activities of the Ag@MSCs using various sizes and concentrations were measured by the colony counting and SAL methods with two types of bacteria and phages (Figure 3). Compared to OH@MSC, the highest concentration (7.13×10^9 particles/ml) of 10, 20, and 30Ag@MSCs exhibited strong inhibition effects, which were statistically significant ($p<0.05$). Additionally, the antimicrobial capabilities of all Ag composites had a similar concentration-dependent tendency. However, 7.13×10^7 particles/ml, the lowest concentration, for the three types of Ag@MSC did not show any strong inhibition effects against the target microorganisms.

Among the 3 types of Ag@MSCs, the 30Ag@MSCs showed the strongest antimicrobial capabilities, inhibiting almost 99% of the *E.coli and B.subtilis* cells, 30% of the MS2 phage particles, and 57% of the ΦX174 phage particles within 1 hr. Moreover, generally, the bacteriophage MS2 showed more resistance to Ag@MSCs than the other microorganisms. Even though the highest concentration (7.13×10^9 particles/ml) for the 10 and 20 Ag@MSCs was treated, the titers for MS2 were the same as the control.

To reveal the relationship between the reaction time and the antimicrobial effect of the Ag composites, each microorganism was treated with 7.13×10^9 particles/ml of the composites at various time points (Figure 4). The results showed that a longer reaction time with Ag@MSCs had a greater effect with a significant reduction in microorganisms, with the exception of MS2.

30Ag@MSCs showed the strongest antimicrobial effects even 3 and 6 hr after the initial treatment.

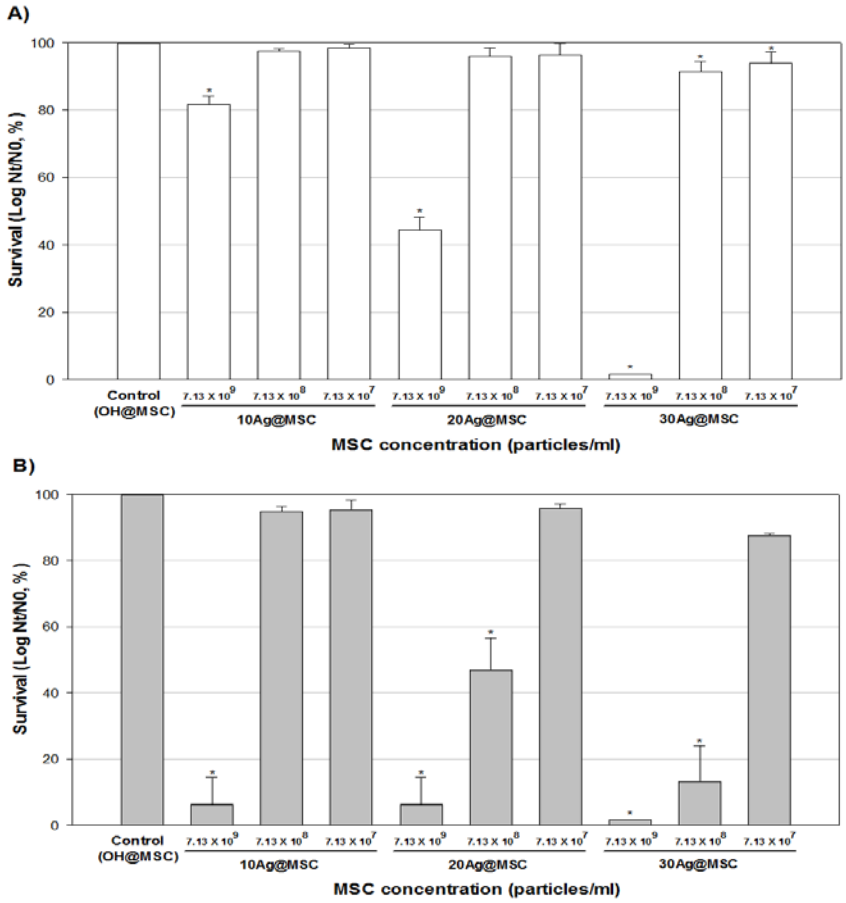

Figure 3.

Antimicrobial effects of Ag@MSCs depending on the various concentrations, A) *E. coli* CN13; B) *B. subtilis*; C) bacteriophage MS2; D) bacteriophage ΦX174. Each microorganism was treated with various concentrations of Ag@MSCs and OH@MSCs (control, 7.13 X 10^9 particles/ml) in a shaking incubator (1 hr, 25℃, 150 rpm). Subsequently, the colony counting (for bacteria) and plaque assay methods (for bacteriophage) were used to measure the surviving microorganisms, expressed as the mean (%) ± standard deviation (SD) compared to the control. Each graph shows the result of three independent experiments and the asterisks indicate a statistical significance. ($p<0.05$; one-way ANOVA with Dunnett's test for multiple comparisons)

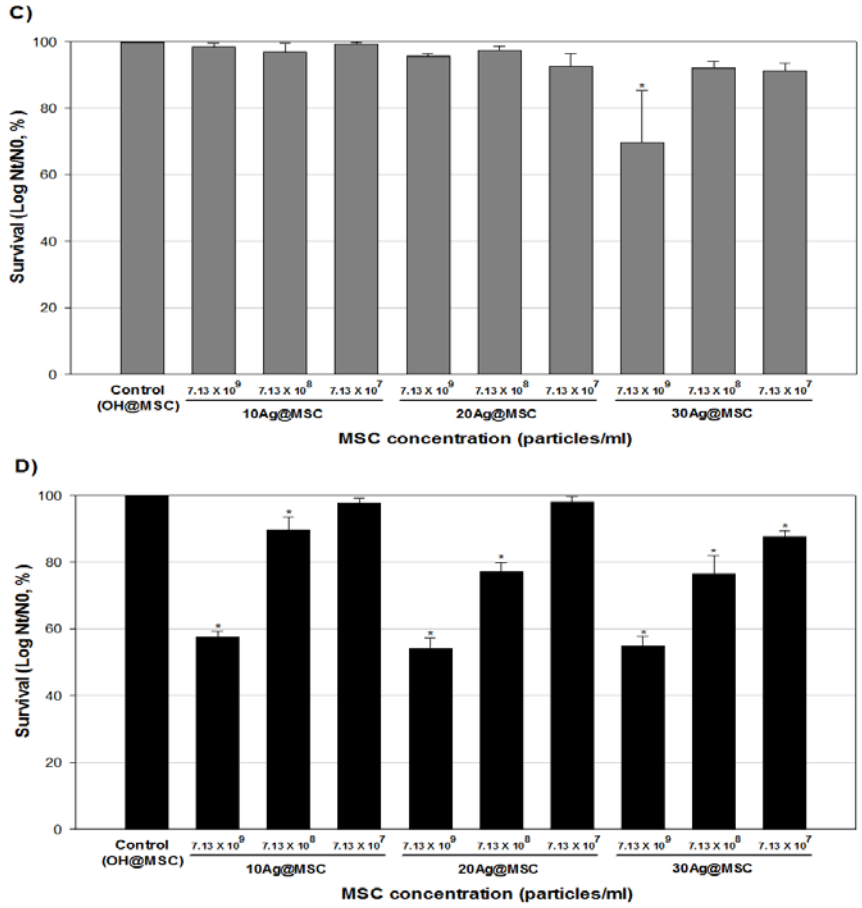

Figure 3. ***(Cont.)***

Antimicrobial effects of Ag@MSCs depending on the various concentrations, A) *E. coli* CN13; B) *B. subtilis*; C) bacteriophage MS2; D) bacteriophage ΦX174. Each microorganism was treated with various concentrations of Ag@MSCs and OH@MSCs (control, 7.13 X 10^9 particles/ml) in a shaking incubator (1 hr, 25℃, 150 rpm). Subsequently, the colony counting (for bacteria) and plaque assay methods (for bacteriophage) were used to measure the surviving microorganisms, expressed as the mean (%) ± standard deviation (SD) compared to the control. Each graph shows the result of three independent experiments and the asterisks indicate a statistical significance. ($p<0.05$; one-way ANOVA with Dunnett's test for multiple comparisons)

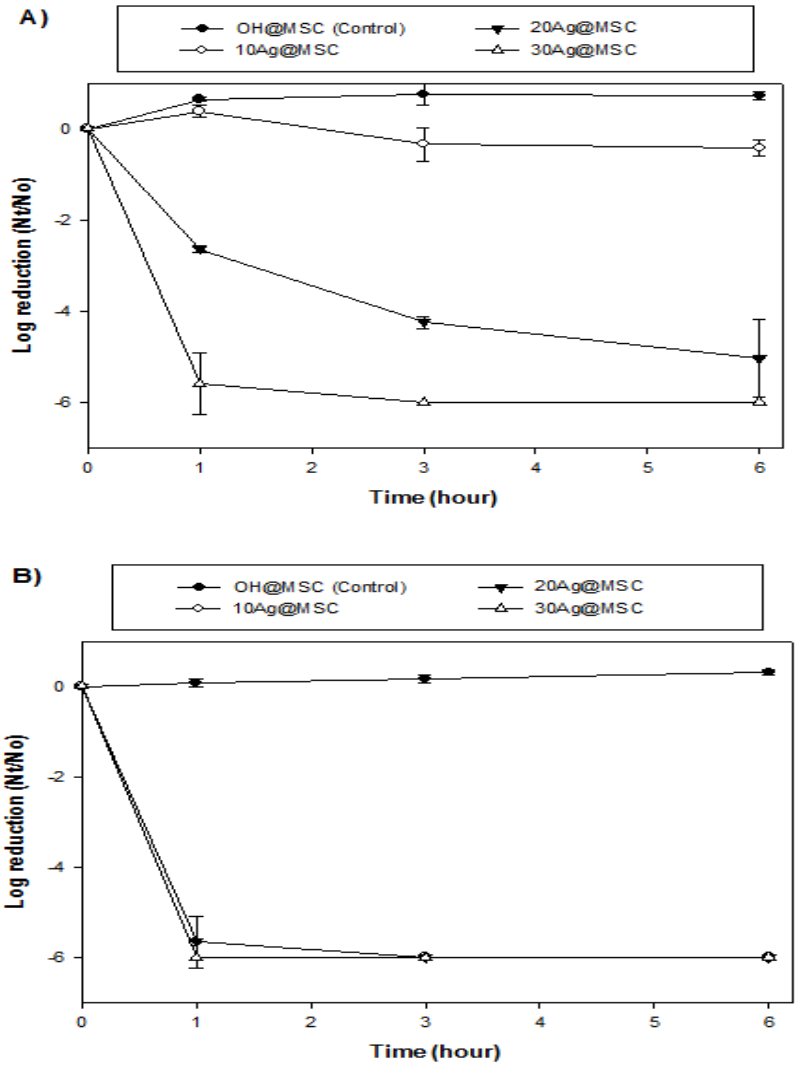

Figure 4.

Antimicrobial effects of Ag@MSCs depending on the various reaction times, A) *E. coli* CN13; B) *B. subtilis*; C) bacteriophage MS2; D) bacteriophage ΦX174. Each microorganism was treated with 7.13 X 10^9 particles/ml of Ag@MSCs and OH@MSCs (control) in a shaking incubator (25℃, 150 rpm). After 1, 3 and 6 hr of incubation, the surviving microorganisms were measured by the colony counting and plaque assay methods, expressed as the mean ± standard deviation (SD). Each graph displays the results of three independent experiments.

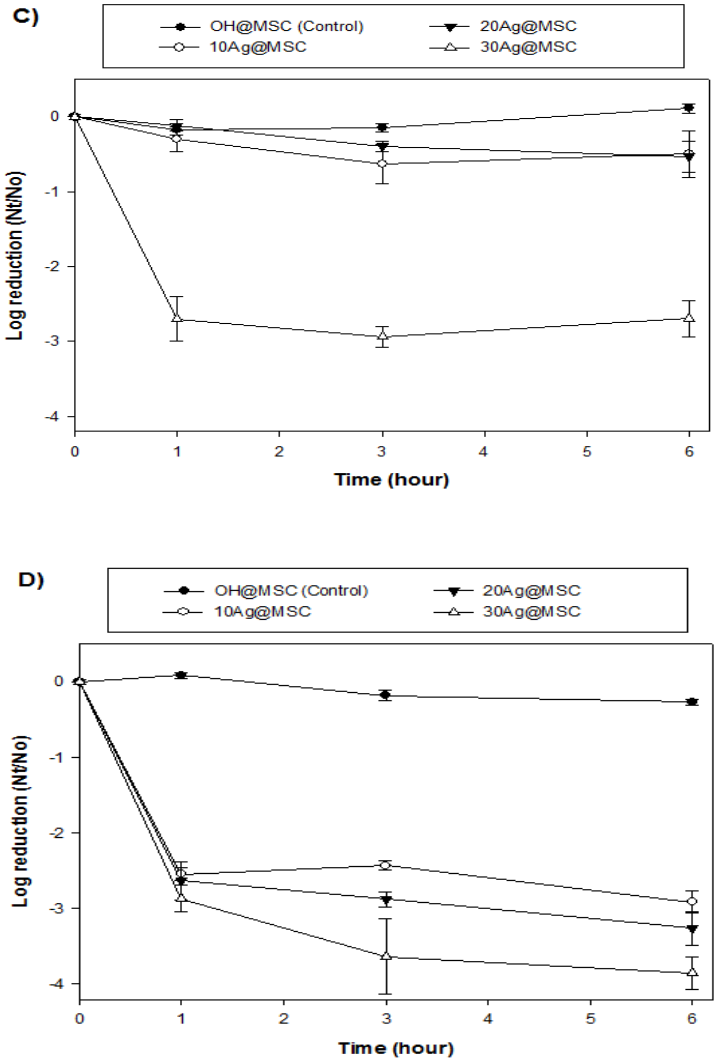

Figure 4. ***(Cont.)***

Antimicrobial effects of Ag@MSCs depending on the various reaction times, A) *E. coli* CN13; B) *B. subtilis*; C) bacteriophage MS2; D) bacteriophage ΦX174. Each microorganism was treated with 7.13 X 10^9 particles/ml of Ag@MSCs and OH@MSCs (control) in a shaking incubator (25℃, 150 rpm). After 1, 3 and 6 hr of incubation, the surviving microorganisms were measured by the colony counting and plaque assay methods, expressed as the mean ± standard deviation (SD). Each graph displays the results of three independent experiments.

2. Effect of exposure to various pH conditions towards Ag@MSCs

Although extreme pH conditions that included pH 2.0 and pH 12.0 were used, 30Ag@MSCs were able to inhibit growth by approximately 6 log CFU/ml of *E.coli* CN13 *and B.subtilis* (data not shown). However, extremely acidic conditions (pH 2.0) reduced the antiviral capabilities of 30Ag@MSCs significantly (Figure 5). After 10 min of exposure to pH 2.0 conditions, the 30Ag@MSCs merely had a 0.1-log reduction in MS2 phage particles and a 0.8-log reduction in ΦX174 phage particles, which were statistically significant compared to the control ($p<0.05$). Exposure to the strong alkali condition (pH 12.0) also affected the inactivation of MS2, showing a 0.7-log reduction after 1 hr treatment.

TEM images of the 30Ag@MSCs to pH 2.0 and pH 12.0 conditions were taken to show the status of the acid- or alkali-treated Ag@MSCs (Figure 6). After treatment at pH 2.0 for 10 min, the TEM image showed that a large number of AgNPs located at the surface of the Ag composites were removed by the strong acid. For the alkali-treated Ag@MSCs, the TEM image showed that there was no external difference compared to the control.

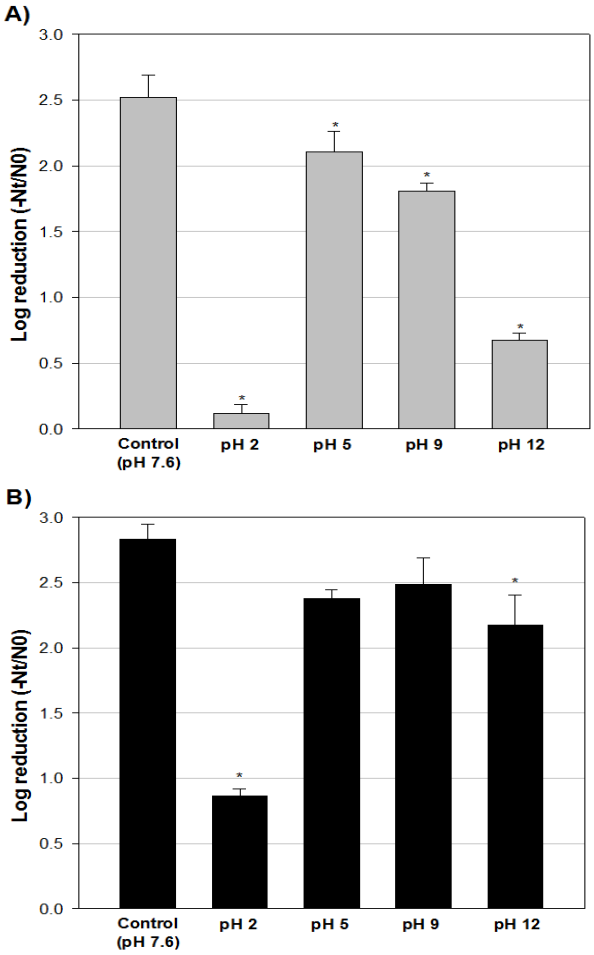

Figure 5.

The Antimicrobial activities of the 30Ag@MSCs after exposure to various pH conditions, A) bacteriophage MS2; B) bacteriophage ΦX174. Prior to treatment with the target microorganisms, 30Ag@MSCs were exposed to acid (pH 2.0 and 5.0) and alkali (pH 9.0 and 12.0) conditions adding 0.1N HCL or 0.1N NaOH in a shaking incubator (10 min, 25℃, 150 rpm), After the acid or alkali were neutralized, the target microorganisms were reacted with the exposed and unexposed (control, pH 7.6) 30Ag@MSCs in a shaking incubator (1 hr, 25℃, 150 rpm). Each graph shows the mean ± standard deviation (SD) of the microorganism concentration of three independent experiments and the asterisks indicate a statistical significance. ($p<0.05$; Kruskal-Wallis one-way ANOVA with Dunnett's test for multiple comparisons)

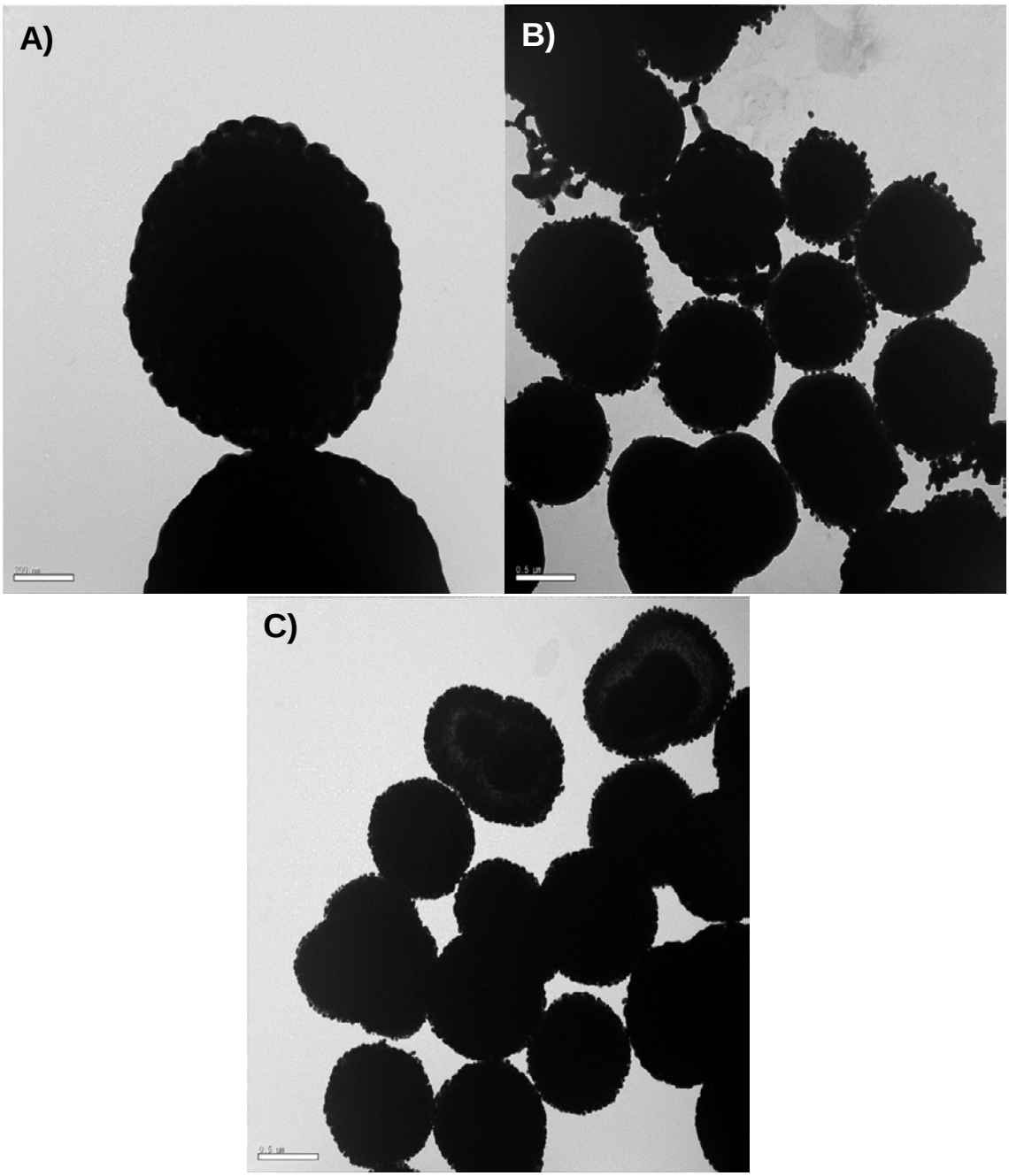

Figure 6.

TEM images of the 30Ag@MSC samples after exposure to various pH conditions, A) Control (pH 7.0); B) Acid (pH 2.0)-treated 30Ag@MSCs; C) Alkali (pH 12.0)-treated 30Ag@MSCs

3. Antimicrobial activities of Ag@MSCs in tap and surface water

The results of the water examination according to Korean standards for drinking water quality revealed that the surface water samples were unfit for drinking due the following quality standards not being met: total colony counts, total coliforms, *Escherichia coli*/Fecal coliforms, and turbidity. Moreover, even tap water samples contained several ions and metals, which could reduce the antimicrobial capabilities of the Ag@MSCs (Table 2).

After exposure to tap and surface water for 1 hr, the 30Ag@MSCs inactivated approximately 6 logs CFU/ml of *E. coli* CN13 *and B .subtilis* (data not shown). Nevertheless, the 30Ag@MSCs removed almost 1.6 logs PFU/ml of MS2 in surface water (non-filtered) conditions, and, were significantly lower than the control ($p<0.05$) (Figure 7). In addition, even though it was not statically significant, the ΦX174 result in surface water (non-filtered) condition was just a 2.3-log reduction, which was considerably lower than the control (over a 2.7-log reduction). Tap and surface water (filtered) conditions reduced the effects of the Ag@MSCs in inhibiting MS2 as well.

Table 2. Results of the water examination[a] for tap and surface water samples according to Korean standards for drinking water quality

Contaminant	Standard (Korea)	Tap water	Surface water (Han river)
Total colony counts	100 CFU/ml	ND	4700*
Total coliforms	ND/100ml	ND	Detected*
Lead (Pb)	0.01 mg/ L	ND	ND
Fluoride (F)	1.5 mg/ L	ND	ND
Arsenic (As)	0.01 mg/ L	ND	ND
Selenium (Se)	0.01 mg/ L	ND	ND
Mercury (Hg)	0.001 mg/ L	ND	ND
Cyanide (CN)	0.01 mg/ L	ND	ND
Hexavalent chromium (Cr^{6+})	0.05 mg/ L	ND	ND
Ammonium Nitrogen (NH_3-N)	0.5 mg/ L	ND	0.09
Nitrate Nitrogen (NO_3-N)	10 mg/ L	2.3	2.0
Cadmium (Cd)	0.005 mg/ L	ND	ND
Phenol	0.005 mg/ L	ND	ND
Trihalomethanes (THMs)	0.1 mg/ L	0.029	ND
Diazinon	0.02 mg/ L	ND	ND
Parathion	0.06 mg/ L	ND	ND
1,2-Dibromo-3-Chloroprapan	0.003 mg/ L	ND	ND
Fenitrothion	0.04 mg/ L	ND	ND
Carbaryl	0.07 mg/ L	ND	ND
1,1,1-Trichloroethane	0.1 mg/ L	ND	ND
Tetrachloroethylene	0.01 mg/ L	ND	ND
Trichloroethylene	0.03 mg/ L	ND	ND
Dichloromethane	0.02 mg/ L	ND	ND
Benzene	0.01 mg/ L	ND	ND
Toluene	0.7 mg/ L	0.006	ND
Ethylbenzene	0.3 mg/ L	0.007	ND
Xylene	0.5 mg/ L	0.011	ND
1.1-Dichloroethylene	0.03 mg/ L	ND	ND
Carbon tetrachloride	0.002 mg/ L	ND	ND

[a] Water analysis was done by Wendi-Bio Inc. (http://www.wendibio.com)

* The contaminants had exceeded drinking water quality standards

Table 2. Results of the water examination[a] for tap and surface water samples according to Korean standards for drinking water quality *(Cont.)*

Contaminant	Standard (Korea)	Tap water	Surface water (Han river)
1,4-Dioxane	0.05 mg/ L	ND	ND
Hardness	300 mg/ L	51	61.0
Consumption of $KMnO_4$	10 mg/ L	0.6	2.6
Odor	odorless (ND)	ND	ND
Taste	tasteless (ND)	ND	ND
Copper (Cu)	1 mg/ L	0.418	0.009
Color	5 (color units)	0	0
Alkyl Benzene Sulfate (ABS)	0.5 mg/ L	ND	ND
pH	5.8~8.5	7.3	7.4
Zinc (Zn)	3 mg/ L	0.079	0.009
Chloride (Cl^-)	250 mg/ L	11	7
Total solids	500 mg/ L	94	87
Iron (Fe)	0.3 mg/ L	ND	0.05
Manganese (Mn)	0.05 mg/ L	ND	ND
Turbidity	0.5 NTU	0.15	6.37*
Sulfate (SO^{4-})	200 mg/ L	9	11
Aluminium (Al)	0.2 mg/ L	ND	0.14
Chlorine residual concentration	4.0 mg/ L	ND	0.48
Boron	1.0 mg/ L	0.01	0.01
Chloroform	0.08 mg/ L	0.02	ND
Escherichia Coli/Fecal coliforms	ND/100ml	ND	Detected*
Chloral hydrate	0.03 mg/ L	ND	ND
Dibromoacetonitrile	0.1 mg/ L	0.0008	ND
Dichloroacetonitrile	0.09 mg/ L	ND	ND
Trichloroacetonitrile	0.004 mg/ L	ND	ND
Haloacetic acid	0.1 mg/ L	0.006	0.006
Bromodichloromethane	0.03 mg/ L	0.006	ND
Dibromochloromethane	0.1 mg/ L	0.003	ND

[a] Water analysis was done by Wendi-Bio Inc. (http://www.wendibio.com)

* The contaminants had exceeded drinking water quality standards

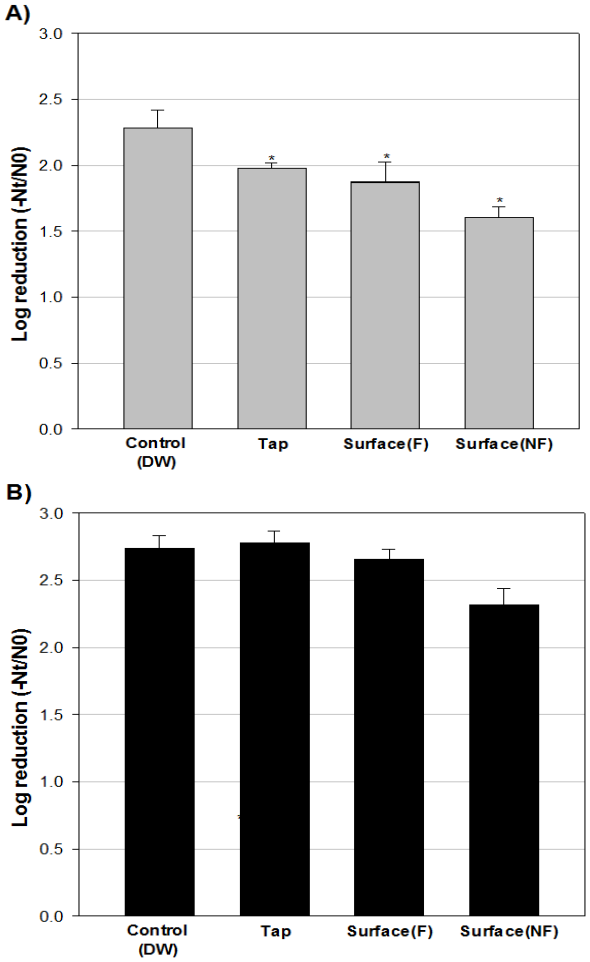

Figure 7.

Inactivation of target microorganisms by 30Ag@MSCs exposed to tap and surface water, A) bacteriophage MS2; B) bacteriophage ΦX174. Before treatment with the microorganisms, the 30Ag@MSCs were exposed to tap water and surface water (F: filtered, NF: non-filtered) from the Han river in a shaking incubator(10 min, 25℃). Subsequently, the target microorganisms were added to the treated and untreated (control) 30Ag@MSCs in a shaking incubator (1 hr, 25℃, 150 rpm). Each graph shows the mean ± standard deviation (SD) of the microorganism concentration of three independent experiments and the asterisks indicate a statistical significance. ($p<0.05$; Kruskal-Wallis one-way ANOVA with Dunnett's test for multiple comparisons)

4. Antimicrobial Mechanisms of Ag@MSCs

A. The relationship between ROS generation and antimicrobial activity.

To understand the effect of ROS induced by the Ag@MSCs, *E.coli* CN13 was treated with 30Ag@MSCs and 1 mM and 0.1 mM of the antioxidant, NAC. When Compared to the control, which exhibited approximately a 6-log reduction in bacteria, 1 mM and 0.1 mM concentrations of NAC had almost a 2.6- and 3.2-log reduction, respectively (Figure 8A).

However, even with incubation of 10, 20, and 30Ag@MSCs, the ROS levels inside the bacteria, measured by the florescence intensity, exhibited a slight increase relative to the control. Bacteria with 30Ag@MSCs had the highest value, around 1.1 fold of the ROS levels, but it was no statistically significant ($p<0.05$) (Figure 8B).

B. Interaction between microbial membrane and Ag@MSCs.

The TEM images of *E. coli* CN13 treated with 30Ag@MSCs for 10 min, 1 hr, and 24 hr revealed the interaction between the bacterial membrane and the Ag composites. After 10 min, most of the bacteria were in contact with the 30Ag@MSCs (Figure 9B). Twenty-four hours later after treatment, the cell membranes were damaged by the Ag composites. The TEM image showed that the cell structure of *E. coli* CN13 was collapsed by the 30Ag@MSCs (Figure 9D).

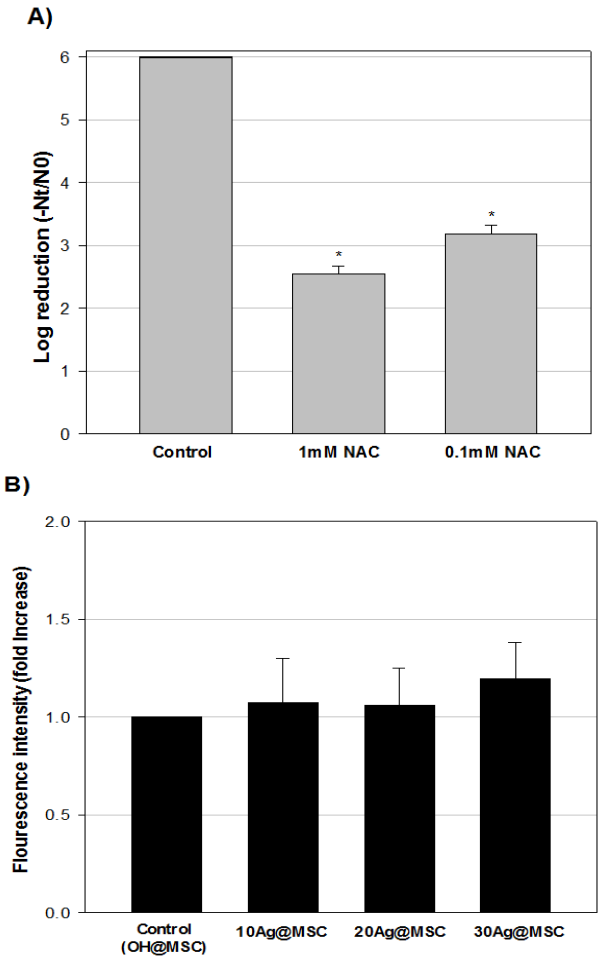

Figure 8.

Antimicrobial effect of reactive oxygen species (ROS) generated by 30Ag@MSCs. A) Approximately $1X10^6$ CFUs/ml of *E. coli* CN13 was treated with 30Ag@MSCs and a certain concentration of the antioxidant N-Acetyl-Cysteine (NAC), in a shaking incubator (1 hr, 25℃, 150 rpm). Each graph displays the mean ± standard deviation (SD) of three independent experiments. B) After incubation with Carboxy-H_2DCFDA (Invitrogen™, USA) for 30 min, *E. coli* CN13 was exposed to 10, 20, and 30Ag@MSCs in a shaking incubator (30 min, 25℃, 150 rpm). The fluorescence of the samples was measured by a microplate reader and the fluorescence intensity was described as the fold increase compared to the control (OH@MSC). Each graph displays the mean ± standard deviation(SD) of six independent experiments. The asterisks indicate a statistical significance. ($p<0.05$; Kruskal-Wallis one-way ANOVA with Dunnett's test for multiple comparisons)

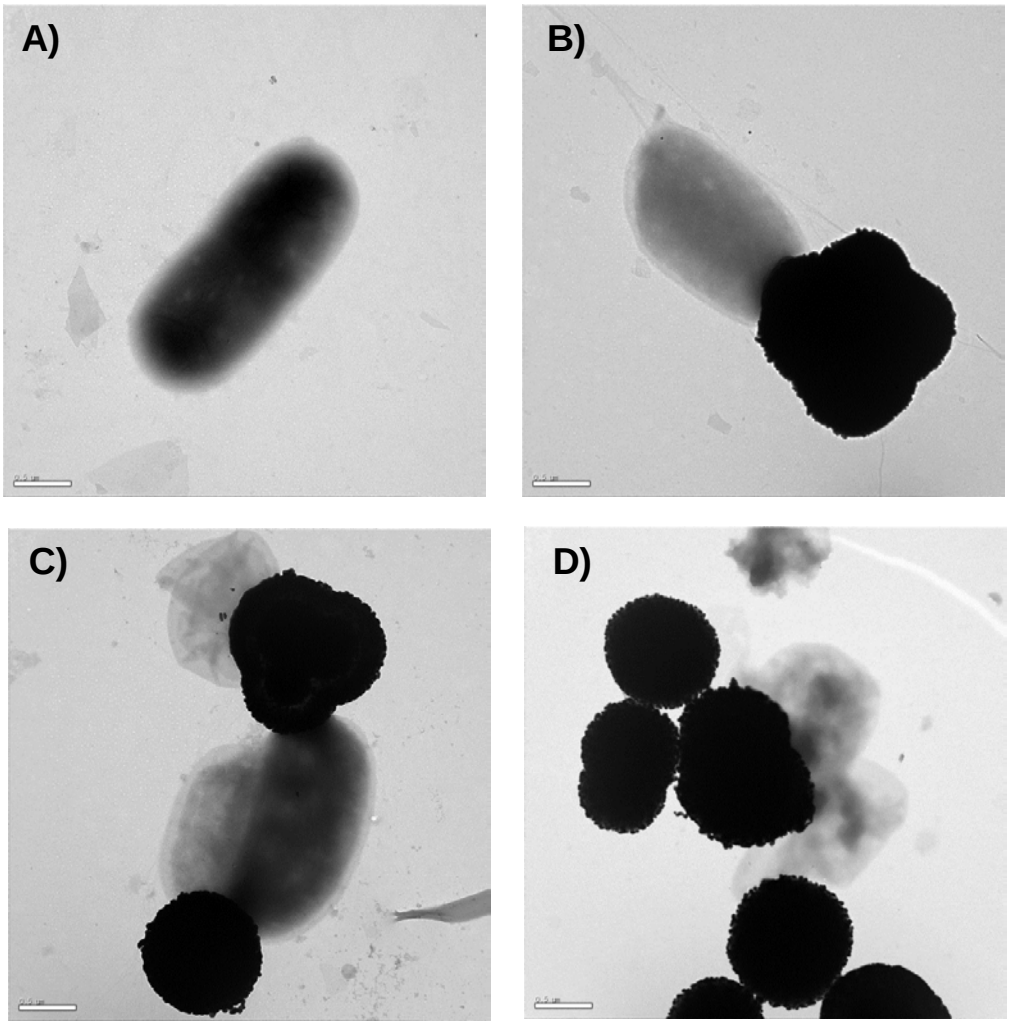

Figure 9.

TEM images of the 30Ag@MSC samples with *E. coli* CN13 at various time points, A) Control; B) After 10min; C) After 1hr; D) After 24hr.

IV. Discussion

Several studies have revealed that the concentration and size of AgNPs are the critical factors to inactivate target microorganisms (1, 9, 13, 27, 32). Generally, according to the literature, AgNPs of a small size show greater antimicrobial capability than larger AgNPs. Moreover, the antimicrobial effects of AgNPs show a concentration-dependent trend. All Ag@MSCs had a similar concentration-dependent tendency after treatment with each target microorganism. However, the 30Ag@MSCs showed the highest level of antimicrobial capabilities, showing greater than 5-log reduction of bacteria and 2-log reduction of phages, compared to the 10 and 20Ag@MSCs. Three important factors affected these results: include the silver concentration in silica layer of each Ag@MSC, the size of the Ag@MSCs, and the surface area of Ag@MSCs. First, there was a difference among the silver concentrations of the Ag@MSCs. 7.13×10^9 particles/ml of 10Ag@MSC and 30Ag@MSC contained 28.75 ppm and 200ppm of silver, respectively. Therefore, although the size of the AgNPs exerts a strong influence on the antimicrobial capabilities of our composites, the 30Ag@MSCs have the greatest effect. Moreover, the size of the Ag@MSCs is almost 500nm as shown in the TEM images (Figure 2). Considering the sizes of the target microorganisms, even bacteria (*E. coli* CN13 and *B. Subtilis)* cannot uptake Ag@MSCs inside their membranes compared to typical monodispersed AgNPs. Consequentially, we assume that the major antimicrobial mechanism of Ag@MSCs is the interaction with the sulfur- or phosphorus- containing biomolecules embedded in the cell membrane or the coat protein. The large size of 10Ag@MSCs interrupts the uptake of 10nm AgNPs, inhibiting their interaction with the biomolecules inside the cell. Lastly, the 20Ag@MSC has the largest surface area, almost 7.35×10^5 nm^2, compared to the surface area of the 10Ag@MSC and 30Ag@MSC

particle. Regardless of a huge difference in the silver concentration between the 20Ag@MSC and 30Ag@MSC, the 20Ag@MSCs showed more than 3-log reduction of bacteria and 2-log reduction of bacteriophage ΦX174. Therefore, we suppose that the surface area of composites is an important factor to affect their antimicrobial capabilities.

Furthermore, this study showed that the antimicrobial capabilities of Ag@MSCs among various microorganisms were clearly different. At first, we chose four target microorganisms, two types of bacteria *(E. coli* CN13 and *B. Subtilis*) and two types of bacteriophages (MS2 and ΦX174) due to the differences in their membrane structures or the types of genes. Even though the 30Ag@MSCs had the strongest antimicrobial effect, the efficacy differences were evident (Figure 3 and, 4). We assume that these results arose due to the specific structure and size of each organism. Gram-positive bacteria have a thick peptidoglycan layer and no outer membrane unlike gram-negative bacteria, which have an outer membrane containing the lipopolysaccharides (LPSs) (15). Also, the diameters of the bacteriophages MS2 and ΦX174 are in both cases 27nm (3, 29), and even *E. coli*, which is rod shaped, is merely 2.0 ㎛ long (17). Additionally, the interaction between the Ag@MSCs and the microorganisms is limited to surface-to-surface reactions compared to the small size of the monodispersed AgNPs, as mentioned above. Given these circumstances, the characteristics of the biomolecules embedded in the outer membranes or proteins can be the critical factors that determine the antimicrobial capabilities of Ag@MSCs. Because the chemical composition of the cell membrane or coat protein of each microorganism is different from the others, the antimicrobial effects of Ag@MSCs among the target microorganisms show a difference as well.

In this study, we evaluated the antimicrobial capacities of 30Ag@MSCs after exposure to

various environmental conditions including the wide ranges of pH, tap water and surface water. First, through the TEM images, we noted that a large number of AgNPs of the 30Ag@MSCs were removed by a strong acid. This affected the efficacy of the 30Ag@MSCs directly. However, for the 30Ag@MSCs, exposure to a strong alkali condition (pH 12.0) led to a loss of efficacy compared to the control, despite the fact that there were no external differences. This result was considered to have arisen due to the 0.1N NaOH, which formulated hydroxide anions (-OH) in the water. Each hydroxide anion bears a negative charge, which allows it to interact with silver easily. Therefore, when Ag@MSCs are exposed to a strong alkali condition, the AgNPs located on the surface of Ag@MSCs react with negatively-charged ions within the solution and lose some of their antimicrobial capability, as some of the AgNPs cannot interact with other negatively-charged molecules embedded in the cell membranes or coat proteins. Moreover, the water samples contained various negatively-charged ions such as sulfate and chloride ions, especially the surface water, which affected the efficacy of the Ag@MSCs. (Table 2). The large number of impurities in the surface water samples was another factor that reduced the antimicrobial capabilities of the Ag@MSCs.

Finally, our results elucidated the antimicrobial mechanisms of Ag@MSCs. First, the TEM images of the 30Ag@MSCs with *E. coli* CN13 revealed that the 30Ag@MSCs were able to interact with the cell membranes (Figure 9). After 24 hours, the cell membrane of *E. coli* was damaged and lost its rod shape completely (Figure 9D). Moreover, after treatment with 30Ag@MSCs and a certain level of antioxidant NAC, the log-reduction of *E. coli* decreased considerably compared to the control. These results suggest that the generated free radical including ROS contributes to the antimicrobial efficacy of 30Ag@MSCs, similar to the study by Kim et al (9). Nevertheless, when we measured the ROS levels inside the *E. coli* after treatment

with Ag@MSCs, there were no significant differences among the Ag@MSCs compared to the control (Figure 8). This result supports that *E. coli* cannot uptake Ag@MSCs due to the large size of the Ag composites and that the main means of inactivation by Ag@MSCs is through interaction with the outer membranes of the target microorganisms. Further study on the topic of AgNP-protein interaction is necessary because the antimicrobial mechanisms of Ag@MSCs are still not completely understood.

In conclusion, the new Ag composites, Ag@MSCs, have excellent antimicrobial capabilities against various microorganisms. Also, even though the bacteria cannot uptake Ag@MSCs inside the membrane, the Ag@MSCs still maintain strong efficacy as monodispersed AgNPs. Moreover, we can recover the Ag@MSCs within a few minutes using a strong magnet to reduce the potential harmful effects on human health and the environment. These results suggest that the AgNP composite can be used in various environmental settings without causing significant human and ecological risks.

V. References

(1) **Ayala Nuñez NV, Lara HH, Ixtepan Turrent L, Rodriguez-Padilla C.** 2009. AgNPs toxicity and bactericidal effect against methicillin-resistant staphylococcus aureus: nanoscale does matter. *Nanobiotechnol.* **5**:2–9.

(2) **Battigelli DA, Sobsey MD, Lobe DC.** 1993. The inactivation of hepatitis A virus and other model viruses by UV irradiation. Wat. Sci. Tech. 27(3-4):339-42.

(3) **Bayer ME, DeBlois RW.** 1974. Diffusion constant and dimension of bacteriophage phi X174 as determined by self-beat laser light spectroscopy and electron microscopy. J Virol. 14(4):975-80.

(4) **Clavero MR, Beuchat LR.** 1996. Survival of Escherichia coli O157:H7 in broth and processed salami as influenced by pH, water activity, and temperature and suitability of media for its recovery. Appl Environ Microbiol. 62(8):2735-40.

(5) **El-Sayed IH, Huang X, El-Sayed MA.** 2005. Surface plasmon resonance scattering and absorption of anti-EGFR antibody conjugated gold nanoparticles in cancer diagnostics: applications in oral cancer. Nano. Lett. 5(5):829-34.

(6) **Epstein H, Afergan E, Moise T, Richter Y, Rudich Y, Golomb G.** 2006. Number-concentration of nanoparticles in liposomal and polymeric multiparticulate preparations: empirical and calculation methods. Biomaterials. 27(4):651-9.

(7) **Hsin YH, Chen CF, Huang S, Shih TS, Lai PS, Chueh PJ.** 2008. The apoptotic effect of nanosilver is mediated by a ROS- and JNK-dependent mechanism involving the

mitochondrial pathway in NIH3T3 cells. Toxicol Lett. 179(3):130-9.

(8) **Hussain SM, Javorina AK, Schrand AM, Duhart HM, Ali SF, Schlager JJ.** 2006. The interaction of manganese nanoparticles with PC-12 cells induces dopamine depletion. Toxicol Sci. Aug;92(2):456-63.

(9) **Kim JS et al.** 2007. Antimicrobial effects of silver nanoparticles. Nanomedicine. 3(1):95-101.

(10) **Lara HH, Ayala-Nuñez NV, Ixtepan-Turrent L, Rodriguez-Padilla C.** 2010. Bactericidal effect of silver nanoparticles against multidrug-resistant bacteria. World. J. Microbiol. Biotechnol. 26:615–621

(11) **Lara HH, Ayala-Nuñez NV, Ixtepan-Turrent L, Rodriguez-Padilla C.** 2010. Mode of antiviral action of silver nanoparticles against HIV-1. J. Nanobiotechnology. 8:1.

(12) **Lara HH, Garza-Treviño EN, Ixtepan-Turrent L, Singh DK.** 2011. Silver nanoparticles are broad-spectrum bactericidal and virucidal compounds. J. Nanobiotechnology. 9:30.

(13) **Lee JE, Zoh KD, Ko G.** 2008. Inactivation and UV disinfection of murine norovirus with TiO2 under various environmental conditions. Appl Environ Microbiol. 74(7):2111-7.

(14) **Lu L et al.** 2008. Silver nanoparticles inhibit hepatitis B virus replication. Antivir. Ther. 13(2):253-62.

(15) **Madican MT, Martinko JM, Dunlap PV, Clack DP**. 2009. Brock Biology of Microorganisms, 12/E**.** Benjamin Cummings.

(16) **Mangoni ML et al.** 2004. Effects of the antimicrobial peptide temporin L on cell morphology, membrane permeability and viability of Escherichia coli. Biochem J. 380:859-65.

(17) **Miao J, Hodgson KO, Ishikawa T, Larabell CA, LeGros MA, Nishino Y.** 2003. Imaging whole Escherichia coli bacteria by using single-particle x-ray diffraction. Proc Natl Acad Sci U S A. 100(1):110-2.

(18) **Mody VV, Siwale R, Singh A, Mody HR.** 2010. Introduction to metallic nanoparticles. J. Pharm. Bioallied .Sci. 2(4):282-9.

(19) **Morones JR et al.** 2005. The bactericidal effect of silver nanoparticles. Nanotechnology. 16(10):2346-53.

(20) **Mukherjee SG, O'Claonadh N, Casey A, Chambers G.** 2012. Comparative in vitro cytotoxicity study of silver nanoparticle on two mammalian cell lines. Toxicol In Vitro. 26(2):238-51.

(21) **Pal S, Tak YK, Song JM.** 2007. Does the antibacterial activity of silver nanoparticles depend on the shape of the nanoparticle? A study of the Gram-negative bacterium Escherichia coli. Appl Environ Microbiol. 73(6):1712-20.

(22) **Park MV et al.** 2011. The effect of particle size on the cytotoxicity, inflammation, developmental toxicity and genotoxicity of silver nanoparticles. Biomaterials. 32(36):9810-7.

(23) **Rai M, Yadav A, Gade A.** 2009. Silver nanoparticles as a new generation of

antimicrobials. Biomaterials. Biotechnol Adv. 27(1):76-83.

(24) **Reeve JN.** 1974. Growth of the Bacillus subtilis cell surface. J Bacteriol. 119(2):560-3.

(25) **Salata O.** 2004. Applications of nanoparticles in biology and medicine. J. Nanobiotechnology. 2(1):3

(26) **Sokolov K et al.** 2003. Optical systems for in vivo molecular imaging of cancer. Technol. Cancer. Res Treat. 2(6):491-504.

(27) **Sondi I, Salopek-Sondi B.** 2004. Silver nanoparticles as antimicrobial agent: a case study on E. coli as a model for Gram-negative bacteria. J.Colloid.Interface.Sci. 275(1):177-82.

(28) **Speshock JL, Murdock RC, Braydich-Stolle LK, Schrand AM, Hussain SM.** 2010. Interaction of silver nanoparticles with Tacaribe virus. J. Nanobiotechnology. 8:19.

(29) **Strauss JH, Sinsheimer RL.** 1963. Purification and properties of bacteriophage MS2 and of its ribonucleic acid. J Mol Biol. 7:43-54

(30) **U.S. EPA.** 2001. Manual of methods for virology: cheater 16. Procedures for detecting coliphages. United States Environmental Protection Agency. U.S.A.http://www.epa.gov/nerlcwww/chapt16.pdf. Accessed 20 April 2012.

(31) **Xu H et al.** 2012. Role of reactive oxygen species in the antibacterial mechanism of silver nanoparticles on Escherichia coli O157:H7. Biometals. 25(1):45-53.

(32) **Yen HJ, Hsu SH, Tsai CL.** 2009. Cytotoxicity and immunological response of gold and silver nanoparticles of different sizes. Small. 5(13):1553-61.

(33) **Zhang Y, Kohler N, Zhang M.** 2002. Surface modification of superparamagnetic magnetite nanoparticles and their intracellular uptake. Biomaterials. 23(7):1553-61.

국문초록

새로운 Magnetic-Silica 은나노 복합체의 미생물 저감 효과

서울대학교 보건대학원
환경보건학과 환경보건학 전공
박 성준

지도교수 고 광표

은나노 입자(AgNPs)는 다양한 미생물을 효과적으로 저감하는 도구로써 많은 관심을 받아왔다. 그러나 은나노 입자의 넓은 부피당 표면적비(surface-to volume ratio)와 세포독성(cytotoxicity)은 다양한 건강문제와 환경오염을 야기시킬 수 있다. 이에 본 연구에서, 우리는 자성 코어(Magnetic core)를 가진 은나노 복합체 (Ag@MSC)를 새로이 고안하였다. 이 새로운 복합체는 자석을 이용하여 수분 내에 회수가 가능하며, 은나노 입자들은 복합체의 실리카 층(silica layer) 표면에 단단하게 결합시켜 강한 충격에도 유실되지 않도록 하였다. 이에 먼저, 분석 대상 미생물로 두 종류의 박테리아(*E. coli* CN13 and *B. Subtilis*) 및 두 종류의 박테리오파지(bacteriophages MS2 and ΦX174)를 선정하여 복합체의 미생물 저감능력을 확인하였다. 또한 새로운 복합체가 처할 수 있는 다양한 환경들을 고려하여, 넓은 범위의 pH 조건과 수돗물, 한강물에 노출 시킨 후의 미생물 저감능력 역시 확인하였다. 10Ag@MSC, 20Ag@MSC 및 30Ag@MSC의 3가지 복합체 중에서, 30Ag@MSC가 가장 높은 미생물 저감능력을 보였다. 7.13×10^9 particles/ml 농도의 30Ag@MSC는 한 시간 반응 후 약 5-log reduction 이상의 박테리아와 2-log reduction 이상의 파지 저감능력을 보였으며, 다양한 환경조건에 노출된 후에도 여전히 강력한 저감 효율을 보여주었다. 결론적으로, 본 은나노 복합체는 다양한 환경조건 안에서 미생물을 적절히 저감하는데 효과적으로 활용할 수 있을 것으로 보이며, 사용 후 손쉽게 회수가 가능하여 여타 은나노 입자 활용의 큰 문제점 중 하나였던 건강적/환경적인 위험을 최소화할 수 있을 것으로 여겨진다.

주요 단어: 은나노입자, 미생물, 나노복합체, 미생물 저감 물질

학번: 2010-23783